

1 Detailed Analysis of Wheat Straw Node and Internode for their Prospective 2 Efficient Utilisation

3 Seyed Hamidreza Ghaffar^{1*}, Mizi Fan¹, Yonghui Zhou¹, Omar Abo Madyan¹

4 *Corresponding author email: seyed.ghaffar@brunel.ac.uk

5 ¹College of Engineering, Design and Physical Sciences, Brunel University London, Uxbridge,
6 Middlesex, UB8 3PH, United Kingdom

7 Key words: Wheat straw, node and internode, physicochemical characterisation, surface chemical
8 distribution

9 Abstract

10 In order to efficiently utilise wheat straw, the systematic examination of their cell wall components,
11 chemical structures, morphology and relation to the physicochemical and mechanical properties is
12 necessary. Detailing of node and internode signifies their different features and characteristics
13 which can ultimately lead to their separated processing for enhanced efficiency and higher added-
14 value bio-refinery. In this study, distinct variations were found amongst characteristics of node and
15 internode, inner and outer surface. It was revealed that node has more extractives, Klason lignin and
16 ash content than internode, higher contents of extractives and ash in the node are related to the
17 thicker epidermis tissue. Hot-water followed by mild steam pre-treatment was used to examine the
18 effects on the characteristics of wheat straw. The results showed: 1) reduced level of waxes and Si
19 (weight %) from the outer surface, and 2) significantly lower ($P < 0.05$) extractives content in both
20 internode and node.

21 1. Introduction

22 Straw is a potential material for the production of bio-products and can present a novel source for
23 the eco-building products such as agricultural compressed fibreboards and bio-composites.

24 Significant studies in the past decade have been carried out to cover a range of applications for
25 wheat straw¹⁻¹⁰. Wheat straw is made up of mainly cellulose, hemicellulose and lignin similar to
26 wood, although it contains less lignocellulose cells with higher amounts of ash and extractive.

27 Wheat straw efficient exploitation for bio-refinery needs the complete characterisation of material
28 science to cover different angles of attributes by detailing the node and internode. It is important to

29 note that not all parts of the agricultural residues are valuable in certain bio-refinery pathways and
30 the undesirable parts must be removed ^{11,12}. Chemical processors and biofuels for instance, need the
31 higher cellulose and hemicellulose parts of biomass. Through differentiation of the details of straw
32 stem, i.e. node and internode, an efficient strategy can be envisaged to optimise the bio-refinery
33 outcome. Controlling the compositional variability of wheat straw is impossible due to their natural
34 source which differs based on the location, growth environment and so on, but it is certainly
35 valuable to screen/monitor the variability and consequently select the specific processing
36 technology for the bio-refinery pathway. In light of the above mentioned point, this research
37 attempts to comprehensively study the internode and node, with inner and outer surface profiles,
38 and track the changes induced by the environmentally combinational pre-treatment. The delivery of
39 a collective wheat straw material science leads to the upgrading of bio-refinery processes, i.e. bio-
40 energy production and bio-product developments, such as bio-composites. The pre-treatment is an
41 essential step to overcome associated issues with wheat straw for bio-refinery pathways intended,
42 for instance to overcome the issues with the surface impeding the good bonding quality, when it
43 comes to the production of straw composite boards.

44 **2. Raw material with analytical characterisation procedures**

45 **2.1 Wheat straw**

46 *Triticum aestivum* L. – wheat straw, was collected in summer from Dixon Brothers Porters Farm,
47 United Kingdom (East of England). The bales were kept in an ambient room temperature for air-
48 dryness. Wheat straw is constituted from internodes, nodes, leaves, chaffs and rachis. The stem of a
49 wheat straw is hollow except for the intermediate growth sections, i.e. nodes which are
50 interconnected via internodes. For different surface characterisation, the node and internode were
51 cut in half longitudinally to expose the outer and inner profiles.

52 **2.2 Pre-treatment**

53 Node and internode samples were additionally selected for pre-treatment to investigate the influence
54 of the pre-treatment on different attributes of the material science and improve their potential

55 pathway for further bio-refinery. The pre-treatment consisted of the following steps: first the
56 samples were placed in a pressure cooker with straw to water ratio of 1:20 (by weight) and a water
57 initial temperature of 100°C (i.e. boiling). After sealing the pressure cooker to maintain a pressure
58 of approximately 0.1 MPa, the internal temperature increased to a maximum of $106 \pm 1^\circ\text{C}$ with
59 advancing of time and pressure. The duration of this stage of pre-treatment was 30 minutes.
60 In the second stage, the straws were taken from the hot water and placed in a mesh basket
61 positioned above hot water inside the pressure cooker, so that the steam at 100°C goes through the
62 straws for another 30 minutes. This completed the environmentally friendly combinational pre-
63 treatment of hot water followed by steam (H+S).

64 **2.3 Tensile test**

65 Three batches were chosen for the tensile testing from the pre-treated and untreated (UN) straws,
66 and from each batch, twenty individual straws were randomly chosen and tested. Therefore, in total
67 for each, pre-treated and UN straw, sixty samples were tested. To reduce the discrepancy of the
68 result, the second node and internode from the root of wheat straw was selected within a length of
69 60 mm. The straw's nodes and internodes were oven dried for 24 hours at 100°C before the testing,
70 to ensure that the different moisture contents do not influence the mechanical strength as previously
71 observed¹³. The 60 mm length of straws was checked thoroughly by microscope for small
72 longitudinal or cross-sectional cuts/defects. The rate used for testing was 5 mm/min using an
73 Instron 2670 series testing machine. Cross sectional area of each sample was carefully measured
74 using a digital caliper.

75 The tensile failure stress σ , of each sample was gathered by using Equation 1.

$$76 \quad \sigma = \frac{F_t}{A} \quad (1)$$

77 Where F_t is the tension force at failure and A is the wall area of the test sample at the failure cross
78 section.

79 **2.4 Chemical analysis and morphology**

80 The straw samples for chemical analysis were made according to NREL/TP-510-42620¹⁴.
81 Moreover, surface chemical distributions (ATR-FTIR) and elemental composition (SEM-EDX) of
82 straws were also examined. Six repetitions were carried out for the wet chemistry (i.e. Klason lignin
83 and extractives content), ten repetitions for surface chemistry (i.e. surface chemical distributions
84 and elemental composition) and the ash content. Table 1 shows the details of each analytical
85 tool/technique chosen.

86 **“Table 1 here”**

87 Attenuated total reflectance-FTIR spectra were recorded on a PerkinElmer Spectrum one
88 Spectrometer. This technique was selected because it permits analysis of the surfaces to a
89 penetrating depth of 0.5-3.0 μm . Wheat straw node and internode were cut in half longitudinally
90 and placed on an ATR equipped with 3 \times bounce diamond crystal with an incident angle of 45° used.
91 In addition to ATR-FTIR, for surface elemental composition analysis, energy dispersive X-ray
92 spectra (SEM-EDX) were obtained using an INCA Energy 400 microanalysis system (Oxford
93 instruments, England). The elements detected were quantitatively analysed using the database of
94 standard samples programmed in the software. Optical microscopy and gun-scanning electron
95 microscopy were both used to assess the morphology of node and internode.

96 **3. Results and discussions**

97 **3.1 Surface chemical functional distribution**

98 The surface chemical functional groups for the node and internode, with the respective, inner and
99 outer surface profiles are illustrated in Fig.1. Table 2 presents the functional groups where the
100 features of different surfaces are compared. In Fig.1 it is observed that there are higher intensity of
101 waxes on the outer surface of the node, reflected by high intensity of 2850 and 2920 cm^{-1} band. The
102 hydrophilic affinity of the inner surface of both the node and internode is reflected by the wide and
103 intense bands in the 3200-3600 cm^{-1} area (Fig. 1a and b), this could be due to the -OH groups

104 present in their main components. It is noteworthy that this characteristic of inner surface could
105 mean that a better interface is achieved when water-based resins are used for straw
106 products/composites.

107 Remarkably, some bands were observed in node but were absent in internode and vice versa,
108 specifically: 2955, 720 and 790 cm^{-1} in node and 985 cm^{-1} in internode, this observation will be
109 interpreted in later part of the paper in connection with wet chemistry examinations.

110 The bands assigned to cellulose at 897 cm^{-1} (asymmetric out-of-phase ring stretch in the C1-O-C4
111 glycosidic linkage), 1372 cm^{-1} (C-H bending), 1429 cm^{-1} (C-H wagging), and 2900 cm^{-1} (C-H
112 stretching) can be selected for quantitative indices evaluation of the cellulose crystallinity¹⁸. The
113 lower order index (LOI) and total crystallinity index (TCI) are gathered based on FTIR spectra¹⁹
114 with the following ratios: TCI (ratio of bands height: $\frac{H_{1372}}{H_{2900}}$) and LOI ($\frac{H_{1429}}{H_{897}}$). Higher values of TCI
115 and LOI translates into higher crystallinity of cellulose^{20,21}. LOI increased by 15% in internode and
116 by 11% in node for H+S pre-treated straws. Moreover, for H+S pre-treated straws, TCI also
117 increased by 24% in internode and by 9% in node. The variation in the cellulose crystalline
118 structure is evident in different anatomical parts, and improvements in the cellulose crystallinity of
119 H+S pre-treated straws means a greater stability to the cellulose chain²², therefore, increase in the
120 mechanical properties such as tensile strength of straw strands.

121 **“Fig. 1 here”**

122 **“Table 2 here”**

123 **3.2 Tensile strength**

124 Tensile strength is chosen to be investigated in this paper as it can govern the mechanical
125 performance of straw composites. A quantitative comparison is designed for the evaluation of the
126 effects of the pre-treatment on the tensile strength of node and internode, shown in Fig. 2. The
127 tensile test results have been verified and show a reliable trend as their coefficient of variance (CV
128 %) for 60 samples ranges from 4.2 to 10%. In the pre-treatment process, it is vital that the fibre

129 structure of straw is not weakened, or else, the mechanical performance of the straw composite will
130 not be satisfactory. The H+S pre-treated straws showed significant increase ($P < 0.05$) of 35% in the
131 tensile strength of internodes and 62% in nodes. The tensile strength of wheat straw node has not
132 been investigated in literature to the best of authors' knowledge. Interestingly, as evident in Fig. 2,
133 the tensile strength of node is significantly lower than internode. This could be related to their
134 morphological properties. In the stem of wheat straw, the node acts as a joint, to provide the
135 connections for the internodes, hence, it does not possess the long stretched longitudinal
136 microfibrils which on the other hand, are the most contributing factor for superior tensile
137 performance of internodes. The node core morphology shown in Fig. 3b (ii), illustrates the compact
138 area occupied by bubbled shape cells, where, the weakest link in node is its core, justifying the
139 lower tensile strength (see Fig. 2). The enhanced tensile strength of H+S pre-treated straws can be
140 due to the higher crystallinity and more ordered structure of cellulose as previously emphasised ⁴.
141 Even though, comparison to other literatures may not be correct, as the origin of straws can
142 influence their characteristics, however, it was found that wheat straw fibres pre-treated via
143 pressurised steam pre-treatment (1MPa for 10 mins) had a tensile strength of 74 MPa ²⁸, that is
144 weaker compared to the H+S pre-treated straws (89 MPa) reported herein.

145 “Fig. 2 here”

146 **3.3 Extractives content**

147 The extractives constitute a heterogeneous set of substances in wheat straw with low molecular
148 weight compounds. The core extractives of wheat straw are sterol esters, resin acids, waxes, fatty
149 acids, triglycerides, fatty alcohols, sterols and a range of phenolic compounds ^{29,30}. Ethanol was used
150 to investigate the lipophilic extractives which can be extracted from wheat straw with organic
151 solvents such as ethanol and acetone ³¹.

152 By looking at Fig. 4a, it is evident that the extractives content in nodes are higher than in internodes
153 for all the cases examined, for example in (hot-water) HW extraction, the node has 10 to 15%

154 higher extractives than internode. This can be related to the sharp band at 720 cm^{-1} , only seen in
155 node outer surface (Fig. 1b), being characteristic of the methylene (CH_2) in-plane deformations
156 rocking²³, and indicating the presence of lipophilic extractives. The difference of extractives
157 content between the node and internode is a confirmation for the results of surface chemical
158 distribution. This feature of higher node's extractives content would be constructive for the
159 selection and process of wheat straw for composites application, as the higher extractives content
160 can have an impeding effect on the optimised interfacial bonding quality between the straw and the
161 water-based resins.

162 A comparison of the extractive yields between HW and the ethanol (ET) extraction shows that HW
163 is a stronger medium of extracting extractives from wheat straw than ET. 10% and 13% higher
164 yields of extractives have been observed for the UN internode and the node respectively.

165 Interestingly, the yield of extractives through HW extraction increases more dramatically for the
166 H+S pre-treated straws by 32% and 27% for internode and node respectively, in comparison to ET
167 extraction. This signifies the dependency of extractives yield on the solvent used for extraction.

168 **3.3.1 Impact of pre-treatment on the extractives content**

169 The extractives in biomass (wood and/or straw) can lead to pitch problems during pulping and
170 papermaking. Sterols and waxes do not form soluble soap in alkaline conditions, i.e. kraft pulping,
171 and therefore, they will be deposited and source pitch problems. The build-up of these extractives
172 can be led to issues for pulp and paper manufacturers³¹, such as technical (reduce the paper strength
173 by interfering with hydrogen bonding during sheet formation) and economic concerns (reduce paper
174 machine efficiency and increase energy consumptions). Removing/weakening the extractives
175 previous to pulping through a pre-treatment of biomass is beneficial for improving the efficiency
176 the bio-refinery pathway.

177 Condensed tannins and phenolics have been shown to be released from the cell structure of wheat
178 straw by the hot water pre-treatment³². Fig. 4a illustrates the lower contents of extractives in H+S

179 pre-treated straws for both HW and ET extraction. HW extraction for H+S straws compared to UN
180 straws has been reduced by 55% and 52%, while, ET extraction has been reduced by 66% and 60%
181 in internode and node respectively. The impact of the H+S pre-treatment on the partial deletion of
182 extractives is also confirmed in the surface chemical functional distribution, as previously observed
183 (Fig. 1). The sharp band at 1739 cm^{-1} on the outer surface of node and internode of UN straws can
184 be assigned to the carboxyl groups in the acids and esters of acetic, ferulic, *p*-coumeric and uronic
185 acids, which have been recognised as core elements of extractives¹. The intensity of this band is
186 diminished after the H+S pre-treatment as evident in Fig. 1. Equally, the strong bands at 2850 and
187 2920 cm^{-1} diminish in intensity for the H+S pre-treated straws. These bands link to the symmetric
188 and asymmetric stretching of the CH_2 -group respectively, which cover the majority of the aliphatic
189 parts of waxes²⁵. In light of the aforementioned, a conclusion is gathered that the extractives in
190 particular waxes (an important group of the lipophilic extractives) have been diminished from node
191 and internode by H+S pre-treatment. Eliminating the wax can be beneficial for wheat straw
192 feedstock, as it facilitates the penetration of pulping chemicals into straw. The H+S pre-treatment of
193 wheat straw has been shown to be a suitable process for dissolution/diminishing of the lipophilic
194 extractives. The removal of nonpolar hydrophobic extractives from wheat straw can, not only
195 improve the wettability which is helpful for composite applications⁴, but also, facilitate the
196 papermaking by decreasing the pitch problems and enhancing paper strength³⁰.

197 **3.4 Klason lignin content**

198 It is shown in Fig. 4b that there is no substantial difference in Klason lignin (KL) content between
199 the HW and ET extracted straws. KL content, however, for HW extracted straws are marginally
200 lower than those of ET extracted straws. The lowest KL content is for HW extracted internode of
201 untreated straws (22%) and the highest is for ET extracted node of H+S pre-treated straws (28%).
202 Generally, the node yielded higher KL content compared to internode, for both untreated and H+S
203 samples, by 15% and 5% respectively, for HW extraction and by 13% and 5% for ET extraction.

204 The greater KL content of node can be clarified in relation to the crystallinity index calculation via
205 X-ray diffraction. In our previous investigation on the same wheat straws, the crystallinity index of
206 node and internode were found to be 35% and 45% respectively ³, this can be an indication of node
207 having more amorphous parts than internode, which is reflected by the higher KL content in the
208 node.

209 **3.4.1 Impact of pre-treatment on the Klason lignin content**

210 The impact of the H+S pre-treatment on the KL content can be seen from Fig. 4b, where there is
211 only a minor upsurge in comparison to untreated straws. The H+S pre-treatment increases the KL
212 content by 18% and 8% for internode and node, respectively, in the case of HW extraction.
213 Similarly, the ET extracted H+S straws; experience an increase in KL content by 12% and 5% in
214 internode and node respectively. The small increase in the amount of KL content for H+S straws
215 can be because of the part deduction of hemicellulose, as high temperature pre-treatments have been
216 proved to remove hemicellulose ³³. Moreover, in chemical functional group distribution (Fig. 1a), it
217 was shown that the lignin bands, particularly at 1510 cm⁻¹, i.e. aromatic ring stretch, are intensified
218 in the case of H+S pre-treated samples. The lignin can be released and re-deposited on the surface
219 as a result of similar pre-treatments to H+S, for instance in the case of hydrothermal pre-treatment
220 of wheat straw ^{34,35} and for the case of steam explosion pre-treatment of aspen wood ³⁶.

221 **3.5 Ash content**

222 Ash content is examined in two forms, i) structural ash and ii) extractable ash. Structural ash is
223 inorganic material that is bound in the physical structure of the biomass whereas extractable ash is
224 inorganic material that can be removed by extraction ³⁷ (in this study by HW and ET).

225 It is observed in Fig. 5 that the node of wheat straw contains more ash, in both pre-treated and
226 untreated non-extracted samples, i.e. the node of H+S pre-treated straws has an ash content of 3.3%
227 compared to the H+S internode of 1.6%, the same values for UN samples are 5.3% and 3.2% (see
228 Fig. 5).

229 In Fig. 4c it can also be seen that for both HW and ET extractions, the node has higher ash content
230 than internode. The higher ash contents of the node can cause problems for the pulping and
231 therefore, removal of nodes prior to pulping will upgrade straw quality as a feedstock. Separation of
232 nodes during collection and storage steps would require modifications of harvesting equipment, or
233 digital image processing ³⁸ or alternatively focus could be on pulping systems ³⁹.

234 In Fig. 4c it is observed that HW extracted samples have less ash remaining than ET extracted
235 samples. In comparison to ET extracted samples, HW extracted ash contents are lower by 40% and
236 32% in UN, and by 13% and 33% in H+S for internode and node respectively.

237 **3.5.1 Impact of pre-treatment on the ash content**

238 The impacts of the pre-treatment on the ash content of wheat straw can present a tremendous
239 opportunity for further successful bio-refinery pathways. Silica constitutes more than 90% of the
240 wheat straw's ash content ⁴⁰. Fig. 5 illustrates a substantial reduction in the ash content of H+S pre-
241 treated straws compared to UN, which is valuable for the composite application as silica inhibits the
242 good quality interfacial bonding ⁴¹. In Fig. 5, it can be seen that for non-extracted H+S straws, the
243 ash content has been reduced by 50% in internode and 38% in node, since 3.2% of UN ash content
244 has been reduced to 1.6% for H+S, and from 5.3% (UN) to 3.3% (H+S), respectively.

245 In our previous investigation on the same wheat straws ⁴, the residual weight calculated based on
246 thermogravimetric analysis (TGA) for untreated straws was higher in comparison to H+S pre-
247 treated straws, i.e. 11% in UN reduced to 4% in the case of internode and 8% in UN reduced to 5%
248 in the case of node, which further approves the partial elimination of ash after the H+S pre-
249 treatment ⁴². Because of the partial removal of extractives and hemicellulose, the H+S pre-treated
250 straws have higher thermal stability and lower ignition residue.

251 **“Fig. 4 here”**

252 **“Fig. 5 here”**

253 **3.6 Surface elemental composition**

254 In Table 3 the elemental composition of wheat straw node and internode with their inner and outer
255 surfaces are tabulated. The elements detected were analysed quantitatively with the use of database
256 of standard samples programmed in the software. The majority of the wheat straw consists of a
257 large amount of carbon (C) and oxygen (O), and a small amount of silicon (Si).

258 Higher amounts of Si weight percentage were found on the outer surface of internode than the inner
259 surface. For untreated straws the internode outer surface had a 5.8% Si weight percentage compared
260 to the inner surface of only 0.8%. On the other hand, the Si weight percentage in H+S internode
261 compared to UN straws was significantly reduced ($P < 0.05$) by 83% and 100% in outer and inner
262 surface respectively. Similarly, the reduction of Si content (weight %) was seen in nodes of H+S
263 pre-treated straws compared to UN, from 2.8 to 0.8% in the outer surface and 0.7 to 0% in the inner
264 surface. The results here for Si weight percentage reduction due to the H+S pre-treatment is
265 reinforced by the substantial reduction of the ash content in H+S pre-treated straws compared to
266 untreated ones as aforementioned in the previous section.

267 When investigating the nodes and internodes, outer to inner surface, it is gathered that more silicon
268 (in the form of silica) is mainly found on the outer surface (i.e. epidermis tissue) of wheat straw.
269 Results for chemical functional groups distribution (Fig.1a and b) further echo this judgment, where
270 the bands of 790 cm^{-1} (Si–C stretching vibration ⁴³) and 985 cm^{-1} (Si–O stretching vibration ⁴³) are
271 only observed on the outer surfaces of node and internode, respectively.

272 In Table 3, it is noticed that the O/C ratio for wheat straw in all locations (anatomical and surfaces)
273 indicates the presence of carbohydrate rich surfaces, as the theoretical O/C ratio of cellulose is
274 reported 0.83 and that of lignin is 0.33 ⁴⁴.

275 **“Table 3 here”**

276 **3.7 Morphology**

277 The epidermis tissue which is on the outermost ring of the wheat straw stem is a cellulose-rich
278 dense layer with a high concentration of silica. This dense layer of epidermal cells provides added
279 mechanical strength to the wheat straw stem. Underneath the epidermis in the internode, a loose
280 layer containing parenchyma and vascular bundles is observed in Fig. 3a, while, the node has a
281 completely different cross sectional morphology, as shown in Fig. 3b. The node possesses a dense
282 zone with closely packed bubbled shaped cells in the middle and elliptical shaped rings well-
283 arranged in a circle, occupying the node core. This morphological difference could indicate the
284 more recalcitrance structure of node compared to the internode, whereby it translates into different
285 physicochemical responses to the pre-treatments and the subsequent enzymatic digestibility ⁴⁵.
286 Heterogeneous morphology counts as one of the important properties of substrate that impacts the
287 enzyme action and activity.

288 **“Fig. 3 here”**

289 The higher content of extractives and ash in nodes than internode (see Fig 4a and Fig. 5) can be
290 related to their morphological characteristics. The thicker epidermis tissue in the nodes i.e. higher
291 content of epidermal cells is mostly composed of the suberized cells and silica cells ⁴⁶, therefore, the
292 ash and extractives contents in the nodes are relatively higher than in the internodes. The epidermis
293 tissue thickness is about 200 µm in the node (Fig 3b (ii)) and about 45 µm (Fig. 3a) in the internode.
294 The H+S pre-treatment impact on the morphological characteristics, as investigated in Fig. 6, apart
295 from a colour change from bright yellow into lighter shade yellow observed during experimentation,
296 is the alterations made to the microstructure. The node's morphology was not subject to a
297 substantial change after the H+S pre-treatment. Conversely, an expansion of parenchyma, (i.e.
298 larger and deeper), in H+S pre-treated internode is observed in Fig. 6a, in comparison to the UN
299 internode as shown in Fig. 6b, that shows a fairly compact zone, arranged closely with smaller
300 circumferences of ellipsoidal honeycomb cells. The expansion of cells could be valuable when it

301 comes to composites production where the resins overflow into the expanded cells, forming
 302 effective entanglement between the straw particles upon solidification. Moreover, the expanded
 303 microstructure can enable the access of the chemical agents and lead to easier fibrillation of wheat
 304 straw for further ethanol process or other bio-refinery pathways of main components of wheat straw,
 305 i.e. hemicellulose and lignin.

306 “Fig. 6 here”

307

308

309

310 Tables

311 **Table 1** - Methods and purpose of investigation for analysis of wheat straw node and internode

Parameters investigated	Methods	Determination
Extractives content	Extracted using two solvents, hot-water (HW) and ethanol (ET), in a soxhlet method for 24 hours following <i>NREL/TP-510-42619</i> ¹⁵ .	i) Examine the different extractives between node and internode, ii) Identify efficient extraction solvent.
Acid insoluble lignin/Klason lignin (KL)	Determined according to <i>NREL/TP-510-42618</i> ¹⁶ . KL determinations were corrected for their relative ash content.	i) Inspect the KL yield in node and internode, ii) The effects of pre-treatment on KL content.
Ash content	According to <i>NREL/TP-510-42622</i> ¹⁷ , the residue after combustion of the organic matter at a temperature of $525 \pm 25^\circ\text{C}$.	i) Classify the ash content of node and internode, ii) The effects of pre-treatment on ash content, iii) Quantify both structural (non-extracted) and extractable ash content.
Surface chemistry	ATR-FTIR spectra were recorded on a PerkinElmer Spectrum one Spectrometer, operated under the following conditions: 4000–650 cm^{-1} range; 4 cm^{-1} resolution; 16 scans.	i) Interpret different surface functionalities in node and internode, ii) Track the changes to the surface chemical distribution after pre-treatment.
Surface elemental	The EDX-SEM spectra were obtained using an INCA Energy 400 microanalysis system.	i) Check the consistency of surface elemental components,

composition		ii) Evaluate the efficiency of pre-treatment in surface modification.
Profile morphology	Investigated using optical microscopy (OM) and field emission gun-scanning electron microscopy (FEG-SEM, Zeiss Supra 35 VP).	i) Differentiation of node and internode, ii) The correlation of morphology and surface chemical characteristics, iii) Changes to morphology induced by pre-treatment.

312

313

314

315

316

317 **Table 2** - Surface functional groups chemical distribution of node and internode

Wavenumber (cm ⁻¹)	Bands assignment	Remarks	Refs.
720	Methylene CH ₂ in-plane deformation rocking	Just seen in the node outer surface	²³
790	Si-C stretching vibration		
985	Si-O stretching vibration	Just seen in the internode outer surface	
1160	C-O-C antisymmetric bridge in hemicellulose and cellulose	Sharper in the internode than the node	
1435	C=O methoxyl group in lignin	Sharper in internode inner surface than outer surface	
1510	C=C lignin aromatic ring stretch	Sharper in the internode of H+S pre-treated straws	²⁴
1739	Carboxyl groups	High intensities in the internode and the node outer surfaces.	¹
2850 & 2920	Symmetric & asymmetric stretching of CH ₂ in aliphatic fraction of waxes	Sharper in the node than the internode and outer than inner surface	²⁵
2955	Asymmetric stretching of CH ₃ in fatty acids	Just seen in the untreated node	²⁶

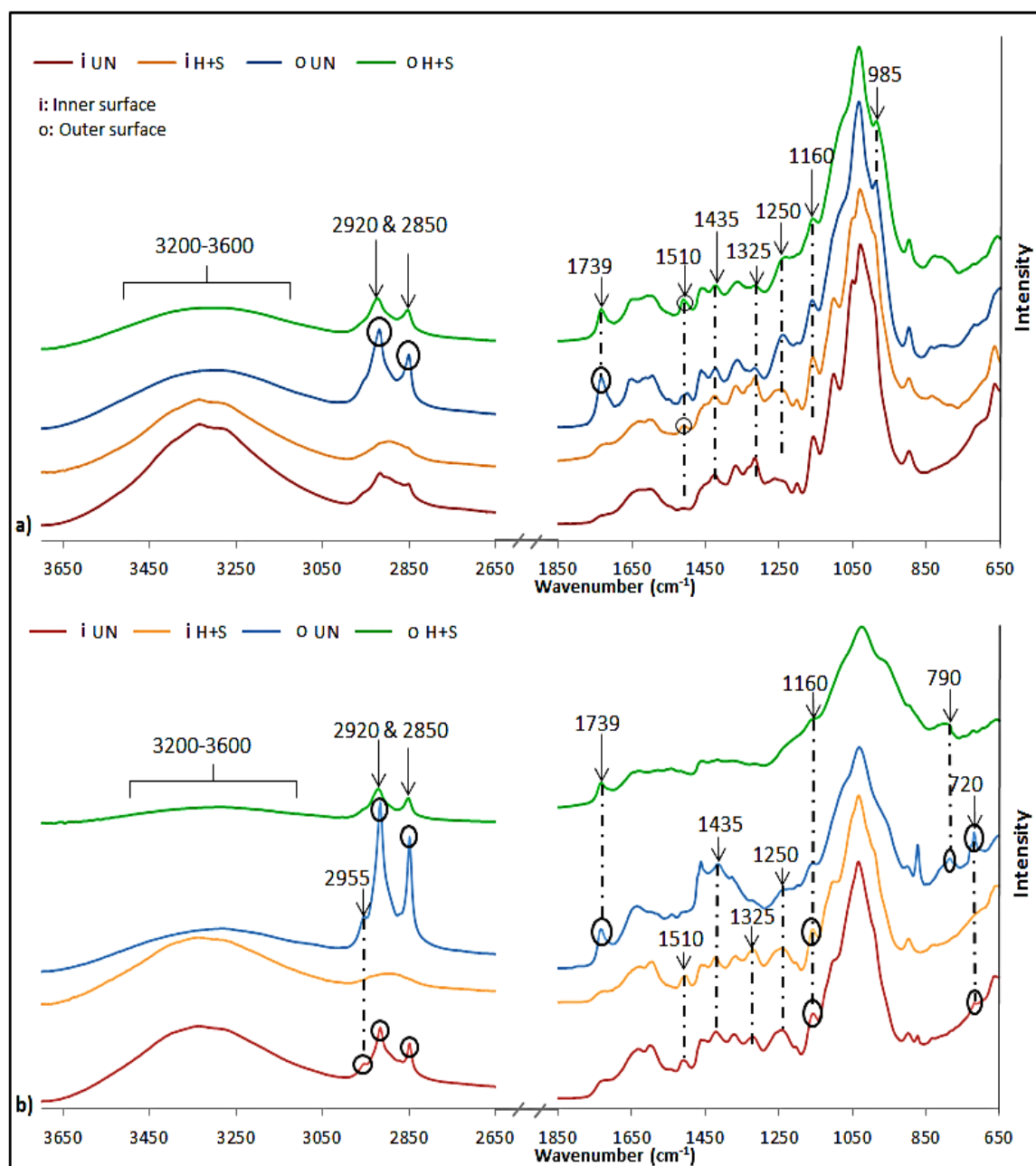
3200-3600 OH stretching of hydroxyl groups Higher intensity in the node and internode of the inner surface than the outer surface

318 **Table 3** - Surface elemental composition of node and internode based on EDX-SEM analysis

Profile Surface	Sample	ID	Percentage %			O/C	
			C	O	Si		
Inner	Internode	UN	54.1 (2)	45 (1)	0.8 (4)	0.83	
		H+S	53.5 (3)	46.4 (7)	0 (1)		0.87
	Node	UN	54.1 (9)	45.6 (7)	0.7 (6)	0.84	
		H+S	53.5 (5)	46.2 (4)	0 (1)		0.86
	Outer	Internode	UN	51.3 (2)	43.4 (5)	5.8 (2)	0.84
			H+S	54.4 (7)	44.5 (3)	1.0 (3)	
Node		UN	53.7 (3)	43.5 (8)	2.8 (2)	0.81	
		H+S	54.5 (2)	44.6 (1)	0.8 (4)		0.82

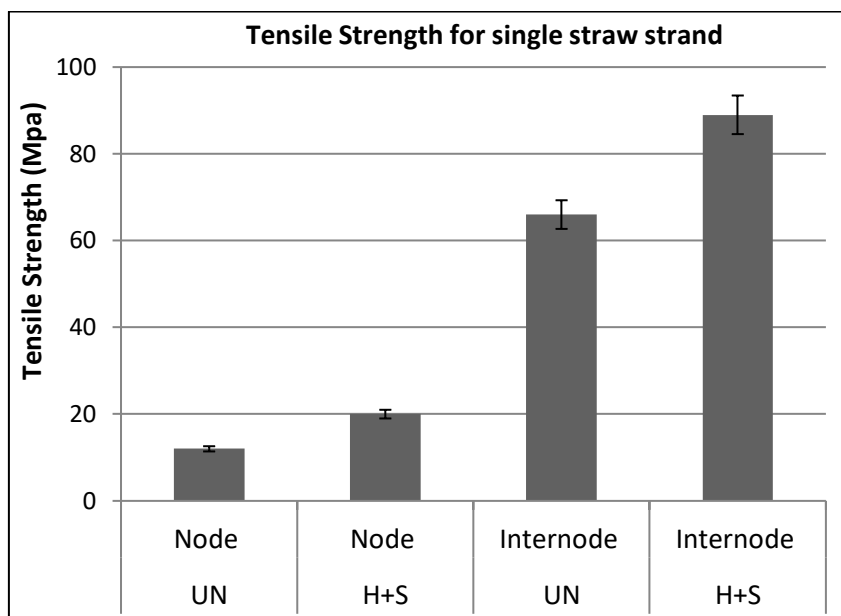
319 *values in () are Coefficient of Variance %

320 **Figures**



321
322
323
324
325

Fig. 1 - ATR-FTIR spectra of a) Internode and b) node of untreated (UN) and pre-treated (H+S) inner and outer surface (Print in colour or see online version for colours)



326
327 **Fig. 2** – Tensile strength of untreated (UN) and pre-treated (H+S) node and internode

328

329

330

331

332

333

334

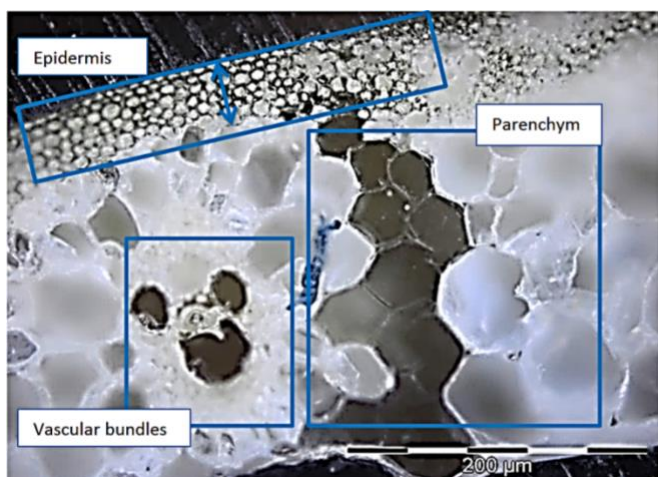
335

336

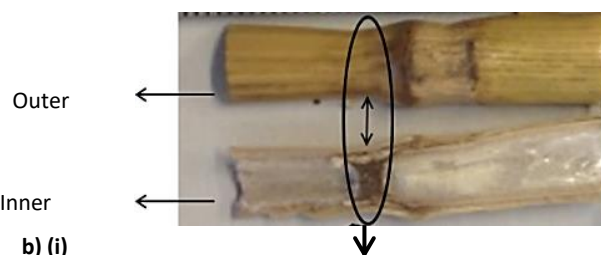
337

338

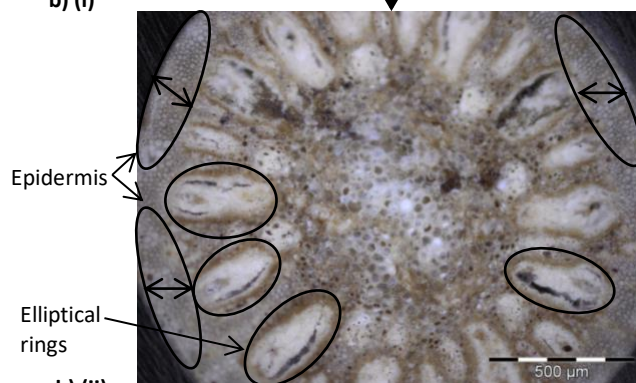
339



340 a)



341 b) (i)



342 b) (ii)

343 **Fig. 3** – a) Cross section of internode; b) (i) Transverse view of node outer and inner surface, and b) (ii) Cross section view of node

344

345

346

347

348

349

350

351

352

353

354

355

356

357

358

359

360

361

362

363

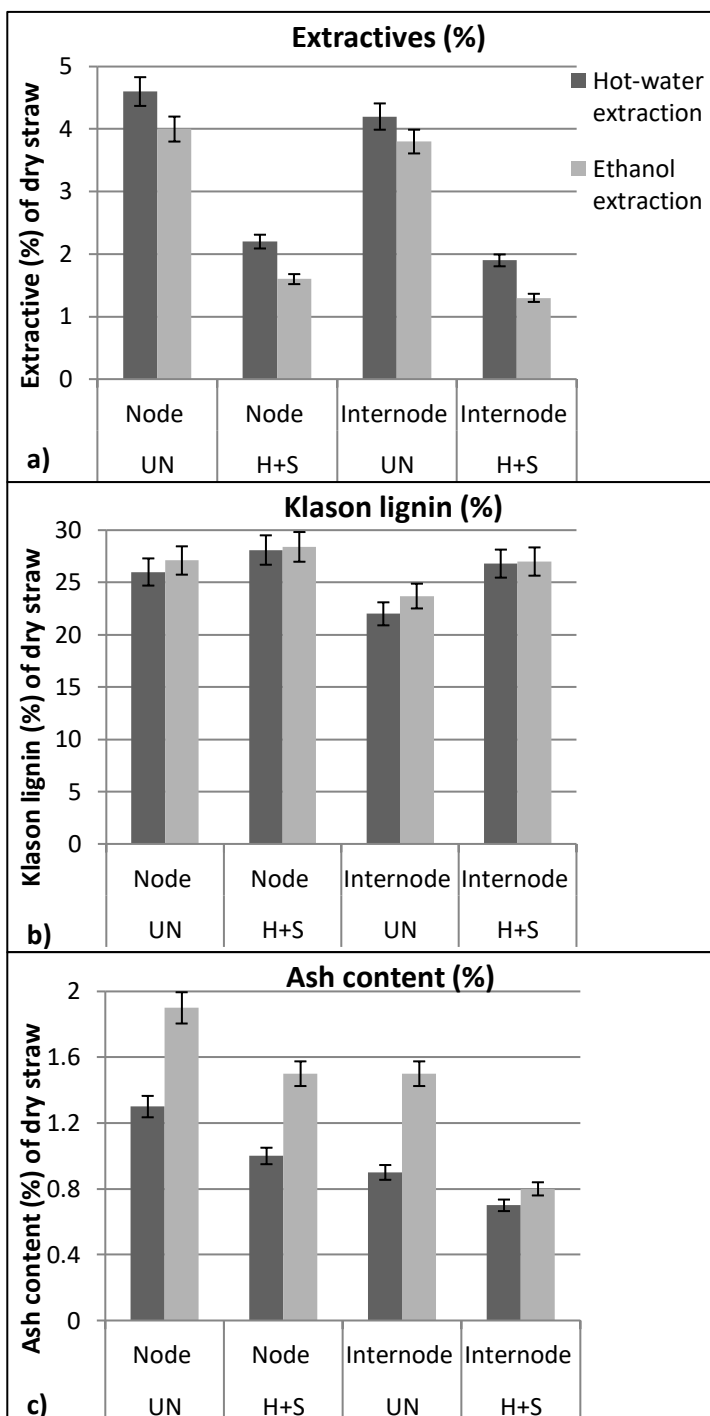
364

365

366

367

368



369

370

371

372

Fig. 4 – Chemical analysis of untreated (UN) and pre-treated (H+S) wheat straw (% dry straw); a) extractives content, b) Klason lignin content and c) ash content of samples with hot-water and ethanol extractions

373

374

375

376

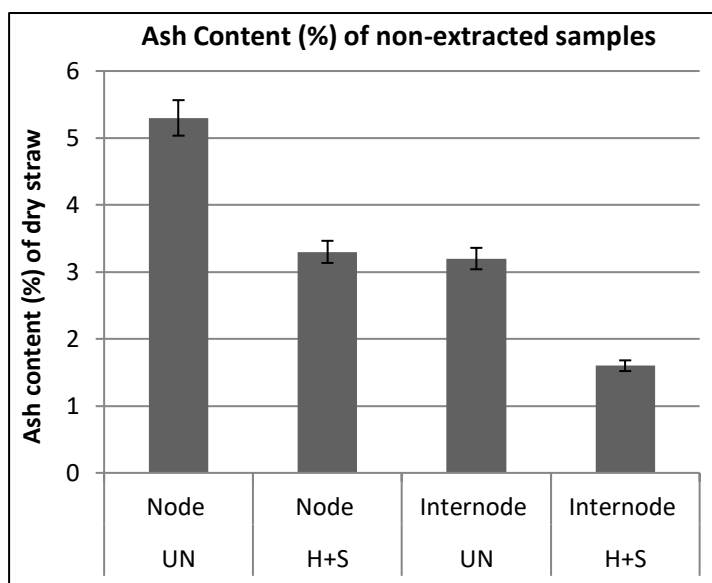
377

378

379

380

381



382 **Fig. 5** – Ash content percentage of non-extracted dry wheat straw for untreated (UN) and pre-treated (H+S)
383 samples

384

385

386

387

388

389

390

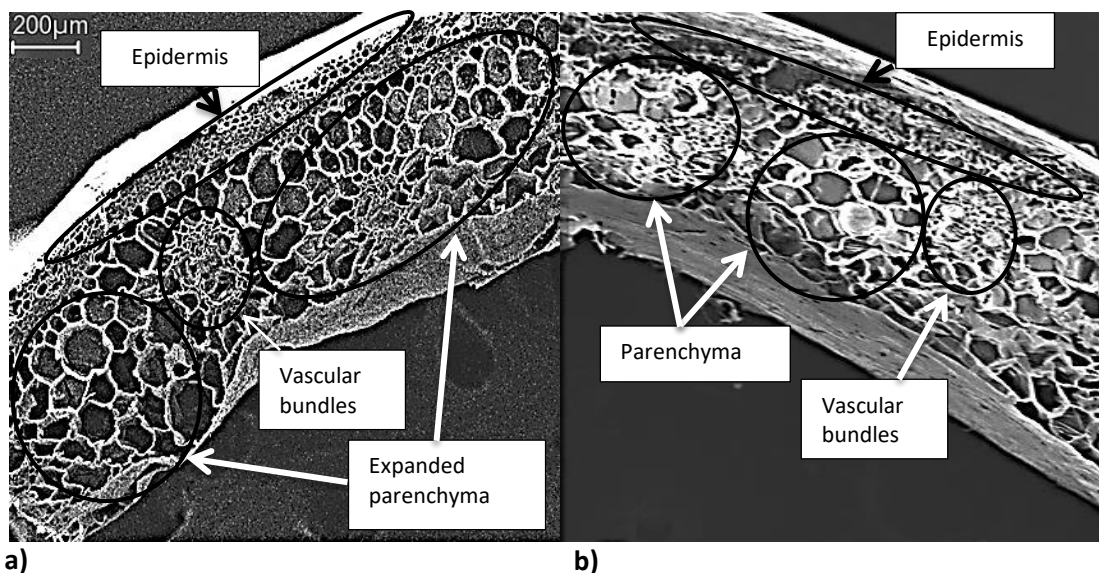
391

392

393

394

395



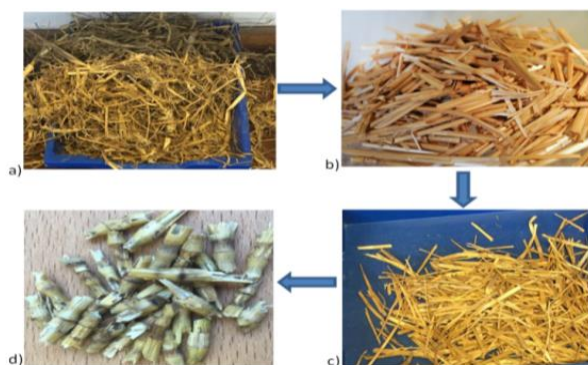
396 **Fig. 6-** SEM micrographs for cross sections of a) pre-treated internode and b) untreated internode

397

398

399 **TOC Graphic**

400
401
402
403
404
405



406 **Graphic Abstract:** Segregation of node and internode for efficient and smart utilisation of straw
407 biomass in bio-refinery

408 (This is to confirm that the TOC Graphic is original and was created by the corresponding author
409 using images taken by corresponding author.)

410

411

412

413

414

415

416

417

418 **References**

- 419 1. Alemdar, A.; Sain, M. Isolation and characterization of nanofibers from agricultural residues –
420 Wheat straw and soy hulls. *Bioresour. Technol.* **2008**, *99*, 1664-1671.
- 421 2. Ghaffar, S.H. 11 - Straw fibre-based construction materials, In *Advanced High Strength Natural*
422 *Fibre Composites in Construction*, Fan, M. and Fu, F., Eds.; Woodhead Publishing: London , 2017;
423 pp. 257-283.
- 424 3. Ghaffar, S.H.; Fan, M. Revealing the morphology and chemical distribution of nodes in wheat
425 straw. *Biomass Bioenergy* **2015**, *77*, 123-134.
- 426 4. Ghaffar, S.H.; Fan, M. Differential behaviour of nodes and internodes of wheat straw with
427 various pre-treatments. *Biomass Bioenergy* **2015**, *83*, 373-382.
- 428 5. Ghaffar, S.H.; Fan, M.; McVicar, B. Bioengineering for utilisation and bioconversion of straw
429 biomass into bio-products. *Industrial Crops and Products* **2015**, *77*, 262-274.
- 430 6. Ghaffar, S.H.; Fan, M. Lignin in straw and its applications as an adhesive. *Int J Adhes Adhes*
431 **2014**, *48*, 92-101.
- 432 7. Ghaffar, S.H.; Fan, M. Structural analysis for lignin characteristics in biomass straw. *Biomass*
433 *Bioenergy* **2013**, *57*, 264-279.
- 434 8. Halvarsson, S.; Edlund, H.; Norgren, M. Manufacture of non-resin wheat straw fibreboards.
435 *Industrial Crops and Products* **2009**, *29*, 437-445.
- 436 9. Halvarsson, S.; Edlund, H.; Norgren, M. Properties of medium-density fibreboard (MDF) based
437 on wheat straw and melamine modified urea formaldehyde (UMF) resin. *Industrial Crops and*
438 *Products* **2008**, *28*, 37-46.
- 439 10. Motte, J.-.; Escudié, R.; Beaufils, N.; Steyer, J.-.; Bernet, N.; Delgenès, J.-.; Dumas, C.
440 Morphological structures of wheat straw strongly impacts its anaerobic digestion. *Industrial Crops*
441 *and Products* **2014**, *52*, 695-701.
- 442 11. Harper, S.; Lynch, J. The chemical components and decomposition of wheat straw leaves,
443 internodes and nodes. *J. Sci. Food Agric.* **1981**, *32*, 1057-1062.
- 444 12. Hess, J.R.; Thompson, D.N.; Hoskinson, R.L.; Shaw, P.G.; Grant, D.R. Physical separation of
445 straw stem components to reduce silica, In *Biotechnology for Fuels and Chemicals*, Finkelstein, M.;
446 Davison, B.H.; Springer: Colorado, 2003; pp. 43-51..
- 447 13. O'Dogherty, M.J.; Huber, J.A.; Dyson, J.; Marshall, C.J. A Study of the Physical and
448 Mechanical Properties of Wheat Straw. *J. Agric. Eng. Res.* **1995**, *62*, 133-142.
- 449 14. Hames, B.; Ruiz, R.; Scarlata, C.; Sluiter, A.; Sluiter, J.; Templeton, D. Preparation of samples
450 for compositional analysis. *Laboratory Analytical Procedure (LAP). National Renewable Energy*
451 *Laboratory* **2008**,

- 452 15. Sluiter, A.; Ruiz, R.; Scarlata, C.; Sluiter, J.; Templeton, D. Determination of extractives in
453 biomass. *Laboratory Analytical Procedure (LAP)* **2005**, 1617,
- 454 16. Sluiter, A.; Hames, B.; Ruiz, R.; Scarlata, C.; Sluiter, J.; Templeton, D.; Crocker, D.
455 Determination of structural carbohydrates and lignin in biomass. Golden, Colorado: National
456 Renewable Energy Laboratory; 2010 Jul. *Report N.TP-510-42618* **2011**, 17.
- 457 17. Sluiter, A.; Hames, B.; Ruiz, R.; Scarlata, C.; Sluiter, J.; Templeton, D. Determination of ash in
458 biomass (NREL/TP-510-42622). *National Renewable Energy Laboratory, Golden* **2005**,
- 459 18. Nelson, M.L.; O'Connor, R.T. Relation of certain infrared bands to cellulose crystallinity and
460 crystal latticed type. Part I. Spectra of lattice types I, II, III and of amorphous cellulose. *J Appl*
461 *Polym Sci* **1964**, 8, 1311-1324.
- 462 19. Åkerholm, M.; Hinterstoisser, B.; Salmén, L. Characterization of the crystalline structure of
463 cellulose using static and dynamic FT-IR spectroscopy. *Carbohydr. Res.* **2004**, 339, 569-578.
- 464 20. Cao, S.; Aita, G.M. Enzymatic hydrolysis and ethanol yields of combined surfactant and dilute
465 ammonia treated sugarcane bagasse. *Bioresour. Technol.* **2013**, 131, 357-364.
- 466 21. Ninomiya, K.; Kamide, K.; Takahashi, K.; Shimizu, N. Enhanced enzymatic saccharification of
467 kenaf powder after ultrasonic pretreatment in ionic liquids at room temperature. *Bioresour. Technol.*
468 **2012**, 103, 259-265.
- 469 22. Xiao, L.; Lin, Z.; Peng, W.; Yuan, T.; Xu, F.; Li, N.; Tao, Q.; Xiang, H.; Sun, R. Unraveling the
470 structural characteristics of lignin in hydrothermal pretreated fibers and manufactured binderless
471 boards from *Eucalyptus grandis*. *Sustainable Chemical Processes* **2014**, 2, 1-12.
- 472 23. Jiang, H.; Zhang, Y.; Wang, X. Effect of lipases on the surface properties of wheat straw.
473 *Industrial Crops and Products* **2009**, 30, 304-310.
- 474 24. Xiao, B.; Sun, X.F.; Sun, R. Chemical, structural, and thermal characterizations of alkali-soluble
475 lignins and hemicelluloses, and cellulose from maize stems, rye straw, and rice straw. *Polym.*
476 *Degrad. Stab.* **2001**, 74, 307-319.
- 477 25. Merk, S.; Blume, A.; Riederer, M. Phase behaviour and crystallinity of plant cuticular waxes
478 studied by Fourier transform infrared spectroscopy. *Planta* **1997**, 204, 44-53.
- 479 26. Dodson, J. Wheat straw ash and its use as a silica source. **2011**,
- 480 27. Stelte, W.; Clemons, C.; Holm, J.; Ahrenfeldt, J.; Henriksen, U.; Sanadi, A. Fuel Pellets from
481 Wheat Straw: The Effect of Lignin Glass Transition and Surface Waxes on Pelletizing Properties.
482 *BioEnergy Research* **2012**, 5, 450-458.
- 483 28. Han, G.; Cheng, W.; Deng, J.; Dai, C.; Zhang, S.; Wu, Q. Effect of pressurized steam treatment
484 on selected properties of wheat straws. *Industrial Crops and Products* **2009**, 30, 48-53.
- 485 29. Sun, R. Extractives, In *Cereal Straw as a Resource for Sustainable Biomaterials and Biofuels*,
486 peng, P., Bian, J. and Sun, R., Eds.; Elsevier: London, 2010; pp. 49-72.

- 487 30. Sun, R.C.; Salisbury, D.; Tomkinson, J. Chemical composition of lipophilic extractives released
488 during the hot water treatment of wheat straw. *Bioresour. Technol.* **2003**, *88*, 95-101.
- 489 31. Sun, R.C.; Tompkinson, J. Comparative study of organic solvent and water-soluble lipophilic
490 extractives from wheat straw I: yield and chemical composition. *Journal of wood science* **2003**, *49*,
491 0047-0052.
- 492 32. Sun, R.; Tomkinson, J. Comparative study of organic solvent-soluble and water-soluble
493 lipophilic extractives from wheat straw 2: spectroscopic and thermal analysis. *Journal of Wood*
494 *Science* **2002**, *48*, 222-226.
- 495 33. Mosier, N.; Hendrickson, R.; Brewer, M.; Ho, N.; Sedlak, M.; Dreshel, R.; Welch, G.; Dien, B.;
496 Aden, A.; Ladisch, M. Industrial scale-up of pH-controlled liquid hot water pretreatment of corn
497 fiber for fuel ethanol production. *Appl. Biochem. Biotechnol.* **2005**, *125*, 77-97.
- 498 34. Kaparaju, P.; Felby, C. Characterization of lignin during oxidative and hydrothermal pre-
499 treatment processes of wheat straw and corn stover. *Bioresour. Technol.* **2010**, *101*, 3175-3181.
- 500 35. Kristensen, J.; Thygesen, L.; Felby, C.; Jorgensen, H.; Elder, T. Cell-wall structural changes in
501 wheat straw pretreated for bioethanol production. *Biotechnology for Biofuels* **2008**, *1*, 5.
- 502 36. Li, J.; Henriksson, G.; Gellerstedt, G. Lignin depolymerization/repolymerization and its critical
503 role for delignification of aspen wood by steam explosion. *Bioresour. Technol.* **2007**, *98*, 3061-
504 3068.
- 505 37. Sluiter, J.B.; Ruiz, R.O.; Scarlata, C.J.; Sluiter, A.D.; Templeton, D.W. Compositional analysis
506 of lignocellulosic feedstocks. 1. Review and description of methods. *J. Agric. Food Chem.* **2010**,
507 *58*, 9043-9053.
- 508 38. Pothula, A.K.; Igathinathane, C.; Kronberg, S.; Hendrickson, J. Digital image processing based
509 identification of nodes and internodes of chopped biomass stems. *Comput. Electron. Agric.* **2014**,
510 *105*, 54-65.
- 511 39. Mckean, W.; Jacobs, R. Wheat straw as a paper fiber source. *Washington, USA: Clean*
512 *Washington Center* **1997**,
- 513 40. Han, G.; Deng, J.; Zhang, S.; Bicho, P.; Wu, Q. Effect of steam explosion treatment on
514 characteristics of wheat straw. *Industrial Crops and Products* **2010**, *31*, 28-33.
- 515 41. Shen, J.; Liu, Z.; Li, J.; Niu, J. Wettability changes of wheat straw treated with chemicals and
516 enzymes. *Journal of Forestry Research* **2011**, *22*, 107-110.
- 517 42. Sun, F.F.; Wang, L.; Hong, J.; Ren, J.; Du, F.; Hu, J.; Zhang, Z.; Zhou, B. The impact of
518 glycerol organosolv pretreatment on the chemistry and enzymatic hydrolyzability of wheat straw.
519 *Bioresour. Technol.* **2015**, *187*, 354-361.
- 520 43. Frost, R.L.; Mendelovici, E. Modification of fibrous silicates surfaces with organic derivatives:
521 An infrared spectroscopic study. *J. Colloid Interface Sci.* **2006**, *294*, 47-52.

- 522 44. Zhao, L.; Boluk, Y. XPS and IGC characterization of steam treated triticale straw. *Appl. Surf.*
523 *Sci.* **2010**, 257, 180-185.
- 524 45. Brienzo, M.; Abud, Y.; Ferreira, S.; Corrales, R.C.N.R.; Ferreira-Leitão, V.S.; Souza, W.d.;
525 Sant'Anna, C. Characterization of anatomy, lignin distribution, and response to pretreatments of
526 sugarcane culm node and internode. *Industrial Crops and Products* **2016**, 84, 305-313.
- 527 46. Carpita, N.C. Structure and biogenesis of the cell walls of grasses. *Annual review of plant*
528 *biology* **1996**, 47, 445-476.
- 529